A Turing Model for Pattern Generation on Lady Beetles

Erik Grandelius

Bachelor's thesis
2016:K8

Faculty of Science
Centre for Mathematical Sciences
Numerical Analysis

Centrum Scientiarum Mathematicarum

Abstract

A Turing model for pattern generation on Lady beetles is considered. This motivates the construction of numerical algorithms for solving reaction-diffusion equations on the sphere. By applying a Galerkin approximation in space, and the implicit Euler method for timestepping, the equation is fully discretized. Convergence orders are proven for this scheme. To obtain a more efficient time stepping algorithm an implicit-explicit splitting is introduced. Some numerical experiments are then performed which demonstrates the superior efficiency of the splitting method. The experiments also verifies the pattern generating ability of the Turing model.

Populärvetenskaplig sammanfattning

En Turing model är en matematisk model i form av en partiell differentialekvation. De introducerades på 50-talet av den brittiska matematikern Alan Turing för att förklara hur biologiska organismer som t. ex. nyckelpigor utvecklar spatiella mönster under sin utveckling. Turing modeller involverar i regel system av olinjära partiella differentialekvationer vars lösning ej kan utryckas med en enkel formel. Istället approximeras lösningen med hjälp av en numerisk algoritm vars fel förhoppningsvis minskar i takt med att beräkningstiden ökar. Det är därför intressant att teoretiskt analysera sådana algoritmer och rigoröst bevisa att de konvergerar mot den exakta lösningen. Dessutom utförs i arbetet numeriska experiment där effektiviteten av ett antal olika algoritmer jämförs. Det visar sej att en så kallad splittringsmetod i detta avseende är ändamålsenlig för ekvationen i fråga.

1 Introduction

In a classical paper [3] dating back to 1952, Alan Turing proposed a general mathematical model for morphogenisis, the pattern formation on animals. The basic idea was that two or more chemical components, so called morphogenes, diffusing at different rates and reacting locally, will under some circumstances self organize into a spatial pattern. This idea was mathematically formalized as a system of semilinear partial differential equations, a reaction diffusion system

$$u_t = D\Delta u + F(u). \tag{1}$$

Here one solves for the vector valued function $u(t,x) = (u_1, ..., u_m)$ which represents the concentration of the various chemicals for a given time and place $(t,x) \in \mathbb{R}^+ \times \mathbb{R}^d$. Most commonly u will have two components but three or more is also feasible in some models. Further, D denotes a diagonal positive definite $m \times m$ matrix representing the diffusion rates of the different components. Finally, $F : \mathbb{R}^m \to \mathbb{R}^m$ is a given nonlinear function which represents the chemical reaction.

Historically Turing models have attracted little interest among biologists, perhaps because it suggests an inherently non-biological solution to a biological problem. It has also been suggested that the mathematics in Turing's original paper was inaccessible for most non mathematicians. However, with the advent of modern molecular biological methods many instances of Turing mechanics has been experimentally verified, see Meinhardt [4].

While reaction diffusion systems were originally introduced as a theoretical model for morphogenisis, they have also been suggested to account more generally for generation of spatial patterns in biological systems. For example Murray [1] successfully applies reaction diffusion models in such diverse areas as cancer tumor spreading and wolf territories.

Even though this type of PDE has been widely applied, the existence and uniqueness of solutions is still not completely understood, see Pierre [10]. This not an uncommon situation for nonlinear PDE's, the Navier-Stokes equation being another obvious example.

Many qualitative properties of reaction diffusion systems can be investigated analytically. These include for example some necessary conditions for "diffusion driven instability", determination of the "wave length" of the solution, stability of stationary states and existence of traveling wave solutions. On the other hand quantitative questions like determining the exact final pattern on a specific domain for a given initial value require numerical simulations.

In Liaw et al. [2] it is proposed that the system

$$\begin{cases} u_t = D_u\Delta u + \rho_0 u^2 v - \mu u \\ v_t = D_v\Delta v - \rho_1 u^2 v + \sigma \end{cases}. \tag{2}$$

solved on a part of the sphere could be a good model for the generation of patterns on various lady beetle species. It is also claimed that the curvature of the sphere is essential for the resulting pattern. By employing a different numerical algorithm for computing the time evolution of the system, a so called *splitting scheme*, we are able to reproduce some of the computations in [2] but with much higher accuracy.

2 Mathematical background

2.1 Problem formulation

With Example (2) in mind we begin our analysis of how to numerically simulate such equations. To facilitate the notation and emphasize the key ideas we will consider a general reaction diffusion system on the 2-sphere, S_2, given by

$$\begin{cases} u_t = D\Delta u + F(u) \text{ in } \Omega' \times [0,T] \\ \hat{n} \cdot \nabla u = 0 \qquad \text{on } \partial\Omega' \times [0,T] \\ u(0,x) = u_0(x) \end{cases}, \tag{3}$$

where Ω' is a subset of S_2, u is a function from $\Omega' \times (0,T]$ to $\mathbb{R}^n$ and $\hat{n}$ is the outward boundary normal of unit length. Moreover D is a positive definite diagonal matrix, Δ denotes the Laplace-Beltrami operator and F is a given (typically nonlinear) function in $C^1(\mathbb{R}^n, \mathbb{R}^n)$. All the differential operators are of course applied component wise.

In order to avoid excessive differential geometric formalism we will fix Ω' to be a part the half sphere and take the usual parametrization

$$(x,y) \mapsto (\sin(x)\cos(y), \sin(x)\sin(y), \cos(x))$$

to pull back (3) to the plane, where it reduces to

$$\begin{cases} u_t = Lu + F(u) \qquad \text{in } \Omega \times (0,T] \\ \hat{n} \cdot \nabla u = 0 \qquad \text{on } \partial\Omega \times (0,T] \\ u(0,x) = u_0(x) \end{cases}, \tag{4}$$

where is L the operator

$$L = D\left(\partial_x^2 + \frac{1}{\sin^2(x)}\partial_y^2 + \frac{1}{\tan(x)}\partial_x\right)$$

and Ω is now a connected open set with smooth boundary at a fixed distance from the singularities at $x = 0$ and $x = \pi$. Thus the main price to pay for a flat domain is that instead of the Laplacian we get the unsymmetric variable coefficient operator L. Crucially however, since we consider the problem on a domain with a fixed distance from $x = 0$ and $x = \pi$, L is still elliptic and shares many key properties with the Laplacian. The disadvantages are mostly of a technical nature; we will have to resort to theoretical results instead of explicit formulae.

In the following H^s is the Sobolev space $W^{s,2}(\Omega \to \mathbb{R}^m)$, the usual $L^2(\Omega \to \mathbb{R}^m)$ inner product is denoted by $\langle \cdot, \cdot \rangle$ i.e.

$$\langle f, g \rangle = \int_\Omega f \cdot g \, dx = \int_\Omega \sum_{i=1}^n f_i g_i \, dx,$$

and the corresponding $L^2(\Omega)$ and $H^s(\Omega)$ norms by $\|\cdot\|$ and $\|\cdot\|_s$ respectively. The Bannach space of continuous functions equipped with the supremum norm will be denoted by $C(\Omega)$. If u is also a function of time we will use the convention that the scalar product or norm acts on the spatial variable only. In the former case it will often be convenient to regard u as a function of time taking values in a Banach space X, i.e. $u(t,\cdot) \in X$. Spaces of

such functions that are continuous or square integrable will be denoted $C([0,T] \to X)$ and $L^2([0,T] \to X)$ respectively.

To use some functional analytic tools such as the Lax-Milgram lemma and energy methods it is advantageous to work with a weak formulation of (4) instead of the classical. It also has the advantage that we are able to deal numerically with the class of weak solutions. Thus we multiply (4) with a test function φ and integrate over Ω. Now, if $u \in C^2(\Omega)$ and $\varphi \in C^1(\Omega)$ then by the Green's theorem

$$\langle Lu, \varphi \rangle = \int_{\partial\Omega} \left[\left(D\partial_x u, D\frac{1}{\sin^2(x)}\partial_y u \right) \cdot \hat{n} \right] \cdot \varphi \, ds - B(u, \varphi), \tag{5}$$

where $B : \left(H^1 \times H^1\right) \to \mathbb{R}$ is the bilinear form given by

$$B(u,v) = \langle D\partial_x u, \partial_x v \rangle + \left\langle D\frac{1}{\sin^2(x)}\partial_y u, \partial_y v \right\rangle - \left\langle D\frac{1}{\tan(x)}\partial_x u, v \right\rangle.$$

We note that somewhat unsatisfactory B is not symmetric, even though the original Laplace-Beltrami operator is symmetric with respect to the scalar product of the sphere. This can be attributed to the fact that our parametrization doesn't scale the two directions on the sphere isometrically, and we are using the unweighted scalar product of the plane. In fact the great Gauss himself showed, as a consequence of his 'Theorema Egregium', that it is impossible to isometrically map an open set of the sphere to an open set of the plane. In view of this result, non-symmetry of the bilinear form B cannot be avoided. We can now state the weak formulation in terms of B:

Definition 2.1. We say that $u \in L^2([0,T] \to H^1)$ with $u_t \in L^2\left([0,T] \to (H^1)^*\right)$ is a weak solution of (2) given that

$$\langle u_t(t), \varphi \rangle + B(u(t), \varphi) = \langle F(u(t)), \varphi \rangle \quad \forall \varphi \in H^1 \text{ and a.e } \ t \in [0,T] \tag{6}$$

and

$$u(0,x) = u_0(x).$$

Here $\langle u_t(t), \varphi \rangle$ is a slight abuse of notation since a general element in the dual of $H^1(\Omega)$ might not be locally integrable. What we mean in the latter case is the functional $u_t(t) \in (H^1)^*$ acting on φ which agrees with our notation if $u_t(t)$ is locally integrable.

The boundary conditions are only implicitly imposed in (6). One can however verify that a weak solution with high enough regularity, say $u \in C^1\left([0,T] \to C^2(\Omega)\right)$, is in fact a classical solution which must satisfy the boundary conditions. This follows from equation (5) by fixing a time t and first consider test functions of compact support. Then the boundary integral vanishes, so that u satisfies (4) in the interior of Ω. But then everything cancels except for the boundary integral so that

$$\int_{\partial\Omega} \left[\left(D\partial_x u, D\frac{1}{\sin^2(x)}\partial_y u \right) \cdot \hat{n} \right] \cdot \varphi \, ds = 0.$$

But if we now consider test functions which are non zero at the boundary we see that u must indeed satisfy the Neumann boundary condition.

2.2 On existence, uniqueness an regularity

What properties do the solutions (4) possess? Do they for example exist? Certainly one does not have global existence in general; the nonlinearity may cause the solution to "blow up" in finite time. Consider for a simple example the scalar equation with

$$F(z) = z^2,$$

and constant initial datum,

$$u(0, x) \equiv 1,$$

in which case (4) reduces to the ODE

$$u' = u^2,$$

with the explicit solution

$$u(t) = \frac{1}{1-t}$$

which clearly blows up as $t \to 1$.

In correspondence with ODE theory however, there is always a unique local solution if F is locally Lipschitz continuous. It is well known that L generates an analytic semigroup, $\{e^{tL}\}$, which yields the solution to the homogeneous linear equation

$$\begin{cases} w_t + Lw = 0 \\ \hat{n} \cdot \nabla w = 0 \text{ on } \partial\Omega \\ w(0, \cdot) = w_0 \end{cases}$$

by the formula $w(t) = e^{tL} w_0$, see Pazy [9]. Furthermore e^{tL} is highly smoothing, in fact $w(t)$ will be in $C^\infty(\Omega)$ for any positive time even if w_0 is only in $L^2(\Omega)$. In particular $\{e^{tL}\}$ preserves the continuous functions, $C(\Omega)$ (see [9], Theorem 7.3.7). There is also an exponential bound on the solution, $\|w(t)\|_{L^\infty} \leq e^{\omega t} \|w_0\|_{L^\infty}$ for some $\omega \in \mathbb{R}$.

Now, by Duhamel's principle any solution of (4) must satisfy the integral equation

$$u(t) = e^{Lt} u_0 + \int_0^t e^{(t-s)L} F(u(s))\, dt. \tag{7}$$

Using this formula and the fact that the semigroup $\{e^{tL}\}$ preserves $C(\Omega)$, it is straight forward to apply the contraction mapping theorem on the space $C([0, T] \to C(\Omega))$. Let the mapping

$$\Phi : C([0, T] \to C(\Omega)) \to C([0, T] \to C(\Omega))$$

be given by

$$\Phi u(t) = e^{tL} u_0 + \int_0^t e^{(t-s)L} F(u(s))\, dt.$$

If T is chosen small enough then Φ is a contraction, mapping some ball around $e^{tL} u_0$ into itself, and thus has a unique fixed point.

The solution thus obtained admits a maximal interval of existence T^*, and persists as long as $\|u(t)\|_{L^\infty}$ stays bounded. Due to the smoothing properties of $\{e^{tL}\}$ the solution will be at least as smooth as F for all positive times in the interval of existence. Quantitatively, for any $\delta > 0$ we have

$$u(t, x) \in C\left([\delta, T] \to C^{k+2}(\Omega)\right) \cap C^1\left([\delta, T] \to C^k(\Omega)\right)$$

if $F \in C^k(\mathbb{R}^n \to \mathbb{R}^n)$, for details see [9].

If F is globally Lipschitz continuous then a simple application of Gronwall's lemma (see [6], appendix B) yields global existence. Observe that we then have $|F(z)| \leq C(1+|z|)$. Now, let T be fixed but arbitrary, and let $A = \max_{t\in[0,T]} \|e^{tL}u_0\|_{L^\infty}$ and $B = \max_{t\in[0,T]} \|e^{tL}\|_{L^\infty}$. Then Duhamel's principle (7) yields

$$\|u(t)\|_{L^\infty} = \|e^{Lt}u_0 + \int_0^t e^{(t-s)L}F(u(s))\,dt\|_{L^\infty} \leq A + \int_0^t BC(1 + \|u(s)\|_{L^\infty}\,ds)$$
$$:= A' + \int_0^t B'\|u(s)\|_\infty\,ds.$$

Thus by Gronwall's lemma

$$\|u(t)\|_{L^\infty} \leq A'e^{B't}$$

so the solution is bounded on $[0,T]$ and hence we have global existence. A similar argument shows the uniqueness of the local solution.

In reality very few interesting reaction-diffusion systems satisfy the global Lipschitz continuity condition, clearly (2) does not. In the crude estimate above we did not pay any attention to the dynamics of the problem. In many systems arising from real chemical reactions however, there is a natural mass-preserving structure. This combined with positivity of the solutions can yield global existence under fairly general assumptions, for a survey see [10].

For the purely mathematical problem of existence and uniqueness a natural class of initial data is L^∞. Indeed, since we do not put any growth condition on the nonlinearity F, $F(u)$ might not even define a distribution if u is essentially unbounded. Conversely, initial data in L^∞ does yield local well-posedness [10]. For numerics on the other hand, it is necessary to require a bit more regularity, $u_0 \in H^s$ with $s \geq 2$, to be able to approximate the initial datum with any order of convergence.

Interestingly enough, while the crude way of handling the nonlinearity by simply estimating it with the Lipschitz constant used above cannot yield global existence in general, convergence of the *numerical approximation* can be proved with the very same technique, given of course that a solution exists. This is because it suffices to consider the numerical solution in a neighborhood of the exact solution, thus it can be truncated outside a bounded set.

3 Constructing a numerical solution

It is common procedure when discretizing time dependent PDE's to discretize the equation in two steps. Firstly, the spatial variable is discretized yielding a large system of ODE's. In our case this means approximating H^1 by a finite dimensional vector subspace which we will denote by S_h and approximating the elliptic operator L by a suitable linear operator L_h acting on S_h[1]. Clearly also F needs to be replaced by a nonlinear operator F_h mapping S_h into itself. Secondly, once the PDE is reduced to the ODE

$$u_t = L_h u - F_h(u) \tag{8}$$

[1] One might make the naive guess L_h should be the restriction of L to S_h but this turns not to be the case. This because for many choices of S_h, L will not map S_h into itself.

for

$$u : \mathbb{R}^+ \to S_h,$$

one may apply any method of choice from the rich toolbox of numerical solutions for ODE's. It is however important acknowledge the special structure of (8), namely the right hand side being the sum two terms. The first term generates a stiff ODE, and the second term nonlinear. The two typically requires different numerical treatment.

3.1 Discretizing the elliptic operator

In accordance with the above remarks we will proceed by discretizing the operator L. We will do this by the so called Galerkin method. This method is not only a computational tool but can also be used as a purely theoretical tool for proving existence of solutions to PDE's, see for example Evans [6]. The basic idea is to in a suitable sense "project the problem" down onto a finite dimensional subspace, replacing the PDE by a large system of ODE's. In the theoretical analysis of the convergence of the Galerkin method, it is not necessary to specify exactly what this subspace is, as long as it approximates the original Sobolev space sufficiently well. Let $\{S_h\}$ be a family of finite dimensional subspaces of H^1 that for some $r \geq 2$ satisfies the following approximation condition:

$$\inf_{\chi \in S_h} \{\|v - \chi\| + h\|(v - \chi)\|_1\} \leq Ch^s \|v\|_s \quad \forall s \leq r. \tag{9}$$

We call the greatest r for which this holds the order of approximation of the family $\{S_h\}$. Such a family of subspaces can be obtained by considering piecewise polynomial functions of degree $r-1$ defined on a triangular grid with maximum perimeter of h, or tensor products of one dimensional splines on a rectangular grid. Proving that the approximation condition (9) indeed holds for these subspaces is a bit technical and we refer to Brenner and Scott [7] Theorem 4.6.11 for details.

The main ingredient in proving convergence (as well as establishing existence) for an elliptic operator is that of coercivity. By employing Poincaré's inequality it is straight forward to show the following Gårding's (see Evans [6], chapter 6) inequality for B:

$$B(v, v) + \kappa \|v\|^2 \geq c_0 \|v\|_1^2 \quad \forall v \in H^1$$

for some $\kappa > 0$. We define $B_\kappa(u, v) = B(u, v) + \kappa \langle u, v \rangle$ and L_κ similarly. It is also clear that B_κ is bounded on H^1:

$$|B_\kappa(u, v)| \leq C\|u\|_1 \|v\|_1.$$

Consider now the stationary elliptic problem

$$B_\kappa(u, \phi) = \langle f, \phi \rangle \qquad \forall \phi \in H^1. \tag{10}$$

By employing Lax-Milgram's lemma [6] one shows that this that equation has a unique solution $Tf \in H^1$ for any $f \in L^2$. By standard elliptic regularity theory ([6], chapter 6) one can show that the solution operator T is actually smoothing by two degrees i.e

$$T \in \mathcal{L}(H^s \to H^{s+2})$$

with the estimate

$$\|Tf\|_{s+2} \leq C\|f\|_s, \tag{11}$$

Thus T is the inverse of L_κ with the Neumann boundary conditions on these Sobolev spaces. Analogously we define the discrete version of T, T_h, by the requirement that

$$B_\kappa\left(T_h f, \chi\right) = \langle f, \chi \rangle \qquad \forall \chi \in S_h. \tag{12}$$

Recall that a finite dimensional linear transformation is invertible if and only if its kernel is trivial. Now if $f \in S_h$, then by the coercivity of B_κ one sees that $T_h f = 0 \Leftrightarrow f = 0$. Hence T_h has an inverse which we will denote by L_h. The following section will clarify why this is a good way of approximating L_κ on S_h.

We now observe that the definition of T_h implies that $T_h f$ is an optimal order approximation to Tf in S_h with respect to the H^1 norm since

$$B_\kappa(T_h f, \chi) = \langle f, \chi \rangle = B_\kappa(Tf, \chi) \qquad \forall \chi \in S_h$$

$$\Longleftrightarrow$$

$$B_\kappa((T_h - T)f, \chi) = 0 \qquad \forall \chi \in S_h.$$

But then we have in particular with $\chi = T_h f$ we get

$$B_\kappa((T - T_h)f, Tf) = B_\kappa((T_h - T)f, Tf - T_h f) \geq c_0 \|(T - T_h)f\|_1^2,$$

by coercivity. On the other hand the boundedness of B yields the upper bound

$$B_\kappa((T - T_h)f, Tf) = B_\kappa((T - T_h)f, Tf - \chi) \leq c_1 \|(T - T_h)f\|_1 \|Tf - \chi\|_1. \qquad \forall \chi \in S_h$$

Thus dividing by $\|(T - T_h)f\|_1$ yields

Lemma 3.1 (Céa's lemma)**.** *The Galerkin solution of the elliptic problem (10) is of optimal order as an S_h approximation to the real solution:*

$$\|(T - T_h)f\|_1 \leq \frac{c_1}{c_0} \inf_{\chi \in S_h} \|Tf - \chi\|_1.$$

Using the smoothing effect of the solution operator T we can obtain optimal order convergence also in the L^2 norm:

Lemma 3.2. *Let S_h have an order of approximation $s \geq 2$. For f in H^{s-2} the operator T_h satisfies the following estimate*

$$\|(T - T_h)f\| + h\|(T - T_h)f\|_1 \leq Ch^s \|f\|_{s-2}.$$

Proof. We first show that $\|(T - T_h)f\|_1 \leq Ch^{s-1}\|f\|$. This follows from immediately from the fact that T_h is a quasi-optimal approximation to T in H^1:

$$\begin{aligned} \|(T_h - T)f\|_1 &\leq C \inf_{\chi \in S_h} \|(\chi - Tf)\|_1 \\ &\leq Ch^{s-1}\|Tf\|_s \leq Ch^{s-1}\|f\|_{s-2}, \end{aligned}$$

where the second inequality is a direct consequence of the approximation condition (3) put on S_h.

Now, let T^* be the solution operator of the adjoint problem so that

$$B_\kappa(\varphi, T^* v) = \langle \varphi, v \rangle \qquad \forall \varphi \in H^1.$$

Evidently the same elliptic regularity theory applies to T^*, i.e. $\|T^* f\|_{s+2} \leq C\|f\|_s$ for $f \in H^s$. In particular we have by setting $\varphi = (T - T_h)f$ in the above equation, $\forall \chi \in S_h$ and $\psi \in L^2$

$$\begin{aligned}\langle (T - T_h)f, \psi \rangle &= B_\kappa[(T - T_h)f, T^*\psi] \\ &= B_\kappa[(T - T_h)f, T^*\psi - \chi] \\ &\leq C\|(T - T_h)f\|_1 \|T^*\psi - \chi\|_1.\end{aligned}$$

Since $T^*\psi \in H^2$ we have

$$\inf_{\chi \in S^h} \|T^*\psi - \chi\|_1 \leq Ch\|T^*\psi\|_2 \leq Ch\|\psi\|.$$

Using this and the previous estimate of $\|(T - T_h)f\|_1$ we obtain

$$\langle (T - T_h)f, \psi \rangle \leq Ch^s \|f\| \|\psi\|.$$

Letting $\psi = (T - T_h)f$ and dividing by $\|(T - T_h)f\|$

$$\|(T - T_h)f\| \leq Ch^s \|f\|,$$

and the lemma is proved.

□

In the calculations above it is convenient to have the term $(T - T_h)f$ "left orthogonal" to S_h with respect to the bilinear form B_κ in the sense that

$$B_\kappa((T - T_h)f, \chi) = 0 \qquad \forall \chi \in S_h.$$

Denoting $R_h := T_h L_\kappa$ one sees that

$$B_\kappa(f - R_h f, \chi) = 0 \qquad \forall \chi \in S_h,$$

and we will refer to R_h as the "elliptic projection". By the previous lemma it is clear that

$$R_h : H^s \to S_h$$

regarded as an approximation operator is of optimal order, in the sense that

$$\|R_h f - f\| + h\|R_h f - f\|_1 \leq Ch^s \|f\|_s. \tag{13}$$

3.2 Semi discrete estimate

We will now define the finite element solution of (6) to be the function $u_h \in C^1([0, T] \to S_h)$ satisfying

$$\langle \partial_t u_h(t), \chi \rangle + B(u_h(t), \chi) = \langle F(u_h(t)), \chi \rangle \quad \forall \chi \in S_h, \forall\, t \in [0, T]. \tag{14}$$

This is clearly the same as requiring u_h to satisfy the ODE (8) with $F_h = P_h F$, P_h being the usual L^2 orthogonal projection.

Since we want to use the elliptic estimates in the previous subsection we somehow have to get around the fact that $B_\kappa \neq B$. This is easily done however by introducing new dependent

variables $\tilde{u} = e^{-t\kappa}u$ and $\tilde{F}(x) = e^{-t\kappa}F(e^{t\kappa}x)$. It should then be clear that u_h satisfies (14) if and only if

$$\langle \tilde{u}_t, \chi \rangle + B_\kappa(\tilde{u}, \chi) = \left\langle \tilde{f}(\tilde{u}), \chi \right\rangle \quad \forall \chi \in S_h \text{ and } \forall t \in [0, T]. \tag{15}$$

We may thus without loss of generality assume that B is coercive, that R_h is the elliptic projection with respect to B etc. The natural question is how accurate an approximation u_h is. The following theorem is proved in the self-adjoint case in Thomée[8]. Observe that we have to put a mild growth condition on the derivative, dF of F.

Theorem 3.3 (Semi Discrete Estimate)**.** *Let u and u_h be defined as in (6) and (14) respectively. Also suppose $\|dF(x)\| \leq C(1 + \|x\|)^p$ for some $p \in \mathbb{R}$. Then*

$$\|u_h(t) - u(t)\| + h\|u_h(t) - u(t)\|_1 \leq C(t)h^r.$$

Proof. For proof consult [8], chapter 14, theorem 2. □

3.3 Convergence of the implicit Euler method

We are now ready to discretize the ODE (14) yielding a fully discrete method. We will analyze the implicit Euler scheme on an equidistant grid with step size k and $t_n = nk$ fixed but arbitrary, so that $n \to \infty$ as $k \to 0$. Introducing the backward difference operator $\bar{\partial}U = (U^n - U^{n-1})/k$, the implicit Euler method can be "implicitly" formulated (no pun intended) by

$$\left\langle \bar{\partial}U^n, \chi \right\rangle + B(U^n, \chi) = \langle F(U^n), \chi \rangle . \tag{16}$$

We will first consider the case when F is globally Lipschitz continuous:

$$|F(x) - F(y)| \leq C|x - y| \qquad \text{for } x, y \in \mathbb{R}^n.$$

It then follows that F as an operator on L^2 is globally Lipschitz continuous:

$$\|F(u) - F(v)\| \leq C\|u - v\| \qquad \forall u, v \in L^2.$$

It is important to note that the next theorem *does not* follow from the well known convergence of implicit Euler in the ODE case. The catch is that the temporal convergence is not allowed to break down as the spatial resolution tends to zero. That is, the constant C is independent of both k and the spatial parameter h.

Theorem 3.4. *The implicit Euler method is first order convergent in time unconditional the spatial discretization i.e. we have the inequality*

$$\|U^n - u(t_n)\| \leq C(h^s + k)$$

for some constant C depending on u and t_n but not on k and h.

Proof. Recall the definition of the elliptic projection R_h in (13) and decompose error as $U^n - u(t_n) = (U^n - R_h u(t)) + (R_h u(t) - u(t_n) := \theta^n + \rho^n$. It then remains to bound the finite dimensional part θ^n. We will proceed with an energy argument. To facilitate notation we will let $w_h^n = R_h u(t_n)$ and $u^n = u(t_n)$.

For any χ in S_h we have

$$\begin{aligned}\left\langle \bar{\partial}\theta^n, \chi \right\rangle + B(\theta^n, \chi) &= \left\langle \bar{\partial}U^n, \chi \right\rangle + B(U^n, \chi) - \left\langle \bar{\partial}w_h^n, \chi \right\rangle - B(w_h^n, \chi) \\ &= \langle F(U^n), \chi \rangle - \langle u_t^n, \chi \rangle - \left\langle \bar{\partial}w_h^n - u_t^n, \chi \right\rangle - B(w_h^n, \chi) \\ &= \langle F(U^n), \chi \rangle - \langle F(u^n), \chi \rangle + B(u^n, \chi) - \left\langle \bar{\partial}w_h^n - u_t^n, \chi \right\rangle - B(w_h^n, \chi).\end{aligned}$$

Since $B(u^n, \chi) - B(w_h^n, \chi) = 0$ this simplifies to

$$\left\langle \bar{\partial}\theta^n, \chi \right\rangle + B(\theta^n, \chi) = \langle F(U^n) - F(u^n), \chi \rangle - \left\langle \bar{\partial}(w_h^n - u^n), \chi \right\rangle - \left\langle \bar{\partial}u^n - u_t^n, \chi \right\rangle, \qquad (17)$$

where we added and subtracted $\left\langle \bar{\partial}u^n, \chi \right\rangle$. Observe now that

$$\left\langle \bar{\partial}\theta^n, \theta^n \right\rangle = \frac{1}{2}\bar{\partial}\|\theta^n\|^2 + \frac{1}{2k}\|\theta^n - \theta^{n-1}\|^2$$

$$\Longrightarrow$$

$$\frac{1}{2}\bar{\partial}\|\theta^n\|^2 \leq \left\langle \bar{\partial}\theta^n, \theta^n \right\rangle.$$

Thus, by setting $\chi = \theta^n$ in (17) and using Cauchy-Schwarz inequality we get

$$\frac{1}{2}\bar{\partial}\|\theta^n\|^2 + B(\theta^n, \theta^n) \leq C\|U^n - u^n\|\|\theta^n\| + \|\bar{\partial}\rho^n\|\|\theta^n\| + \|\bar{\partial}u^n - u_t^n\|\|\theta^n\|,$$

where we also used the Lipschitz continuity of F.

Recall that $U^n - u^n = \theta^n + \rho^n$. Thus, using the elementary inequality $ab \leq \epsilon a^2 + \frac{1}{4\epsilon}b^2$ and the fact that $\|\theta^n\|^2$ is bounded by $B(\theta^n, \theta^n)$ we obtain the "discrete Gronwall's inequality" for θ

$$\bar{\partial}\|\theta^n\|^2 \leq C\|\theta^n\|^2 + \|\bar{\partial}\rho^n\|^2 + \|\bar{\partial}u^n - u_t^n\|^2,$$

and the rest of the proof is straight forward bookkeeping.

Now, evidently the last inequality implies that for sufficiently small k

$$\|\theta^n\|^2 \leq (1 + kC)\|\theta^{n-1}\|^2 + Ck(\|\bar{\partial}\rho^n\|^2 + \|\bar{\partial}u^n - u_t^n\|^2).$$

Inductively we then have

$$\|\theta^n\|^2 \leq (1 + kC)^n\|\theta^0\|^2 + Ck\sum_{j=1}^{n} A_j$$

where $A_j := \|\bar{\partial}\rho^j\|^2 + \|\bar{\partial}u^j - u_t^j\|^2$.

Recall that t_n is fixed and that $k = t_n/n$, thus we estimate the first term by

$$\left(1 + \frac{Ct_n}{n}\right)^n \|R_h v - v\| \leq C' e^{t_n C}\|R_h v - v\| \leq C_1 e^{t_n C} h^s \|v\| := C(t_n)h^s\|v\|_s.$$

By the mean value theorem we have

$$\|\bar{\partial}\rho^j\| \leq \|\frac{1}{k}\int_{t_{j-1}}^{t_j} \rho_t \, \mathrm{d}s\| \leq \frac{1}{k}\int_{t_{j-1}}^{t_j} \|R_h u_t - u_t\| \, \mathrm{d}s \leq C(u)h^s,$$

where we again use the approximation properties of R_h (13) and the regularity of the exact solution, $u_t \in H^s$. In the second term observe that

$$\bar{\partial} u^j - u_t^j = -\frac{1}{k} \int_{t_{j-1}}^{t_j} (s - t_{j-1}) u_{tt}(s) \, \mathrm{d}s,$$

so that consequently

$$\begin{aligned} \|\bar{\partial} u^j - u_t^j\| &\leq \|\frac{1}{k} \int_{t_{j-1}}^{t_j} (s - t_{j-1}) u_{tt}(s) \, \mathrm{d}s\| \\ &\leq \int_{t_{j-1}}^{t_j} \|u_{tt}(s)\| \, \mathrm{d}s \\ &\leq \max_{t_{j-1} \leq s \leq t_j} \|u_{tt}(s)\| k. \end{aligned}$$

By collecting all the terms on the right hand side and applying obvious estimates we have

$$\|\theta^n\| \leq C(t_n) \|v\|_s h^s + C(u) h^s + \max_{0 \leq s \leq t_n} \|u_{tt}(s)\| k,$$

and the statement of the theorem follows. □

The general case when F is not globally Lipschitz continuous can now be dealt with by considering a smooth truncation $\tilde{F}$ of F such that $\tilde{F}(x) = \textit{constant}$ for $x \geq R$. We may then apply the above theorem to conclude in particular that u_h is bounded, let's say $\|u_h\| \leq R/2$, and hence that our truncated function $\tilde{F}$ equals F on the range of u_h and u.

3.4 Splitting methods

We will now consider two alternatives to the implicit Euler method for the temporal discretization. For comparison all three methods are:

Implicit Euler(IE):

$$U_{n+1} = (I - k(L + F))^{-1} U_n$$

Implicit-Explixit(IMEX):

$$U_{n+1} = (I - kL)^{-1}(I + kF) U_n$$

Implicit-Explicit with Dimensional splitting(IMEX-ADI):

$$U_{n+1} = (I - kL_y)^{-1}(I - kL_x)^{-1}(I + kF) U_n.$$

Here, $L_x = \partial_x^2 + \frac{1}{\tan(x)} \partial_x$ and $L_y = \frac{1}{\sin^2(x)} \partial_y^2$ where we for notational convenience have dropped the dependence on h. We will not consider the Explicit Euler scheme since the CFL-condition makes it useless for interesting values of $\frac{\Delta t}{(\Delta x)^2}$ (with this we mean values where the error resulting from the spatial discretization does not completely dominate, see Figure 4.2).

The name "splitting" refers to the fact that the time evolution of L and F are computed separately. Physically this can be interpreted as first allowing the chemical components

react, and then allowing them to diffuse. In general this will not yield the same result as if they were computed simultaneously. Compare with the situation in an autonomous linear system of ODE's:

$$\begin{cases} x' = (A+B)x \\ x(0) = x_0. \end{cases}$$

Here the time evolution is given by the matrix exponential,

$$x(t_n) = e^{nk(A+B)}x_0.$$

But this will not be equal to the splitting

$$\tilde{x}(t_n) = (e^{kA}e^{kB})^n x_0,$$

unless A and B commutes. Thus a *splitting error* is introduced.

From a computational point of view there are three big advantages with the IMEX method compared to IE:

(i) There is no nonlinear equation solving required.

(ii) The linear system, $(I - kL)x = b$, that has to be solved at each time step is invariant of time. Thus a single sparse LU factorization can be done before iterating in time, so that only an upper triangular system has to be solved at each time step.

(iii) The linear system $(I - kL)x = b$ decouples in the components of u. Thus we can compute $(I - kL)u_i^{n+1} = u_i^n$ in parallel for all the components of u. Since the implicit step in generally dominates the computational effort, this reduces the computation time by a factor of $1/m$, where m is the number of components of u.

The advantage of the ADI splitting is that it is possible to get the matrices A_x and A_y approximating L_x and L_y tridiagonal with the right ordering of the basis, and thus the linear system can be very efficiently solved using the Thomas algorithm. However, with the spatial discretization schemes we will use, the matrices A_x and A_y will not commute, resulting in a splitting error. This can be seen in contrast to the dimensional splitting of the planar Laplacian, where A_x and A_y resulting from the same discretization scheme commute, so that the splitting is in fact exact. With our implementation we have observed that the ADI scheme is roughly twice as fast as the IMEX scheme but much more inaccurate.

4 Simulations

In this section we carry out some numerical experiments to complement the theoretical discussion in the previous sections. For our numerical experiments we will consider an "activator-depleted substrate" model provided by Mienhardt [5] given by

$$\begin{cases} u_t = D_u \Delta u + f(u,v) \\ v_t = D_v \Delta v + g(u,v) \end{cases} \tag{18}$$

with

$$\begin{cases} f(u,v) = \rho_0 u^2 v - \mu u \\ g(u,v) = -\rho_1 u^2 v + \sigma \end{cases}. \tag{19}$$

All the above constants are positive. Here D_u and D_v are the diffusion coefficients. Normally D_v needs to be 25-100 times larger than D_u to generate patterns. Intuitively u is locally (in space) consuming the substrate v, while in absence of v it decays exponentially. The substrate v on the other hand is being produced at a linear rate in the absence of u. Since v is assumed to diffuse considerably faster than u, the substrate will be "sucked" into regions where the concentration of u higher. If however such a region where u dominates grows to large, v will not diffuse fast enough to provide "fuel" for u and eventually the negative feedback provided by μ will dominate. As a consequence the region where u dominates will grow a hole or split in two. Of course as we pull the equation back to the plane with our usual parametrization, the Laplacian has to be replaced with the operator L.

With parameters suitably chosen the above solution converges to a stationary state exhibiting striking geometrical dot pattern as seen in Figure 1.

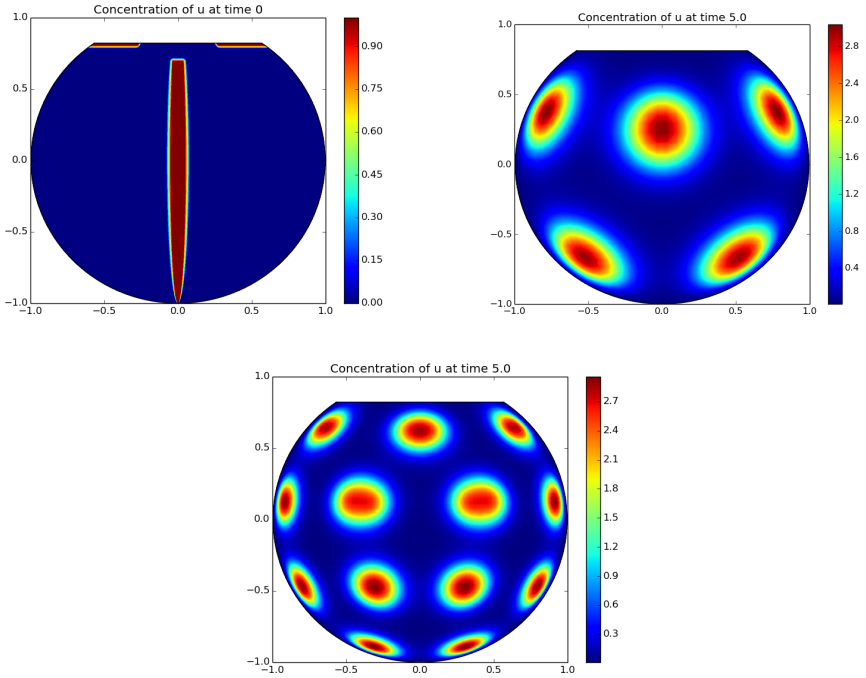

Figure 1: The initial distribution is show in the first image. The five spot patter obtained by solving (18) on a 100x100 grid (with the the spatial discretization described in detail in section 4.1) and the IMEX method in time with a stepsize of $k = 10^{-3}$. The parameters of the model are set to $D_u = 0.18, D_v = 70D_u,\ \rho_0 = 54,\ \rho_1 = 108,\ \mu = 24,\ \sigma = 30$. By lowering the diffusive rates to $D_u = 0.06,\ D_v = 70D_u$, the number of dots increases to thirteen. Here we have plotted the concentration of the activator u. In general the substrate v will exhibit the dual pattern.

By adding a saturation effect in the nonlinearity

$$\begin{cases} f(u,v) = \rho_0 \frac{u^2 v}{1+\kappa u^2} - \mu u \\ g(u,v) = -\rho_1 \frac{u^2 v}{1+\kappa u^2} + \sigma \end{cases} \tag{20}$$

a stripe pattern emerges, as can be seen in Figure 2. Note how the solution evolves as a traveling wave. The final distribution is similar to the striped pattern of the Asian species *macroileis hauseri*.

Interestingly enough it turns out to be relatively difficult to obtain a seven spot pattern with this model and geometric domain, the seven spot *Coccinella septempunctata* being the most common species in Europe. One possible solution could be to split the domain in two and introduce a Neumann condition in the middle. It is outside the scope of this thesis to perform any more systematic study of parameters. We simply give examples of how some basic patterns can be generated. The model could of course be refined in many other ways, for example by considering growing domains, time dependent diffusion rates etc. It is the authors opinion however that such refinements should made in close connection to empirical studies, perhaps by dissecting the beetle in the developmental state.

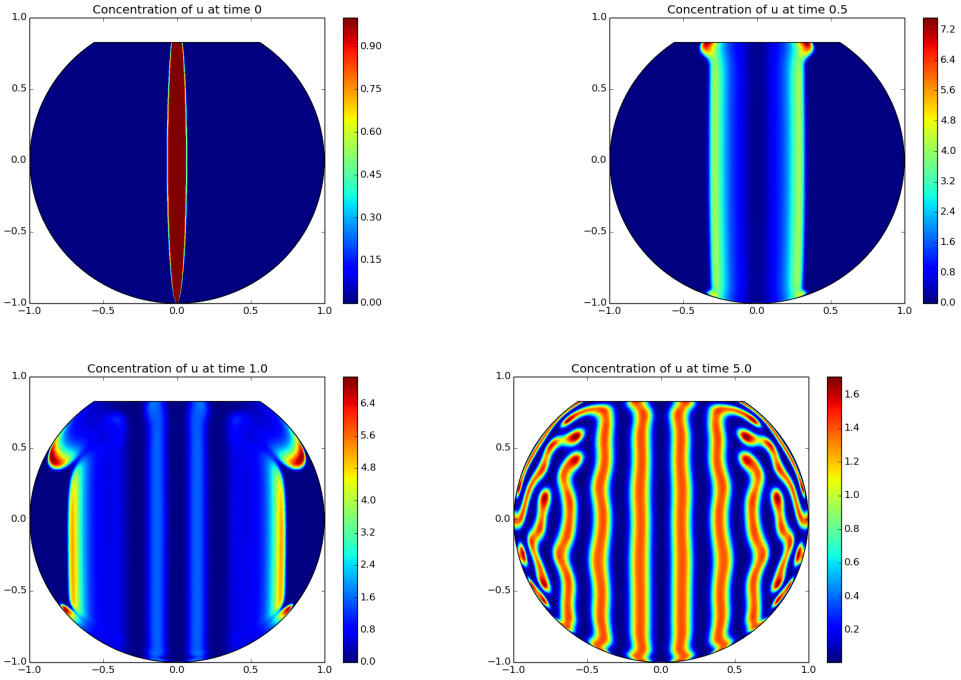

Figure 2: By solving (20) w saturation effect of $\kappa = 0.35$ in we obtain a striped pattern as final distribution. The other parameters are $D_u = 0.06, D_v = 70D_u$, $\rho_0 = 54$, $\rho_1 = 108$, $\mu = 24$, $\sigma = 30$. We use a finer spatial grid than in the previous simulation with a 200×200 grid and the time step size is $kt = 10^{-3}$. Notice how the solution evolves like a travelling wave.

4.1 Implementing the spatial discretization

For our numerical experiments we will for the sake of convenience take the domain Ω to be the square $[x_0, \pi - x_1] \times [0, \pi]$. This domain clearly does not have a smooth boundary so the theory in the first two sections does not directly apply. In particular it is well known that

higher elliptic regularity of the form (11) fails when the domain has corners. The best one can say is that $u \in H^2(\Omega)$ even if f is in $C^\infty(\Omega)$. However, one still has *inner* regularity in the sense that $\|u\|_{H^{s+2}(\Omega')} \leq \|f\|_{H^s(\Omega')}$ for any open Ω' strictly contained in Ω, see [6]. Analogously it is shown in Nitsche et. al. [11] that the Galerkin method still is of optimal order on elements with support strictly contained in the *interior* of the domain. Since we are actually completely uninterested in correctly simulating the potential discontinuities in the corners, we will henceforth be content with measuring the error at interior nodes and treat the domain as if the boundary really was smooth.

Thanks to rectangular domain we can choose a finite dimensional space $\{S_h\}$ that is easy to work with. We take $S_h = S^1 \otimes S^1$, the tensor product of one dimensional linear splines on a uniform rectangular grid of width h. We take as a basis

$$\phi_i(x) \otimes \phi_j(y)$$

where ϕ_i and ϕ_j are one dimensional tent functions centered at $x_{ij} = (x_0 + ih(\pi - 2x_0), jh\pi)$. A typical basis function can be seen in Figure 3.

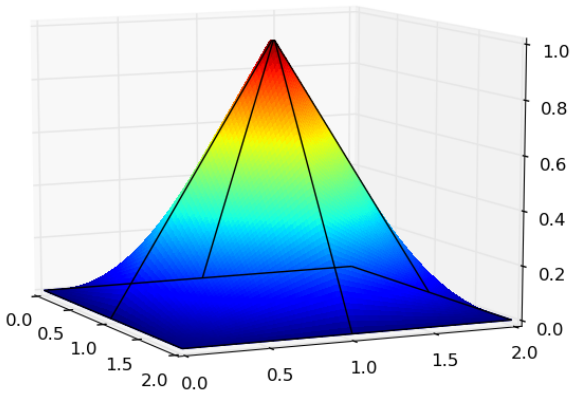

Figure 3: A typical basis function of $S^1 \otimes S^1$. The function being the product of piecewise linear functions is bilinear in each quadrant.

We plug these basis functions into B to obtain the stiffness matrix K:

$$\begin{aligned}
B(\phi_i \otimes \phi_j, \phi_k \otimes \phi_l) &= \langle\, \partial_x\phi_i \otimes \phi_j, \partial_x\phi_k \otimes \phi_l \,\rangle \\
&+ \left\langle\, \partial_y\phi_i \otimes \phi_j, \frac{1}{\sin^2(x)}\partial_y\phi_k \otimes \phi_l \,\right\rangle \\
&- \left\langle\, \phi_i \otimes \phi_j, \frac{1}{\tan(x)}\partial_x\phi_k \otimes \phi_l \,\right\rangle \\
&= \int \partial_x\phi_i\partial_x\phi_k dx \int \phi_j\phi_l dy \\
&- \int \phi_i \frac{1}{\tan(x)}\partial_x\phi_k dx \int \phi_j\phi_l dy \\
&+ \int \frac{1}{\sin^2(x)}\phi_i\phi_k dx \int \partial_y\phi_j\partial_y\phi_l dy \\
&\approx \left(\frac{1}{h}T_{ik} + \frac{1}{\tan(x_i)}S_{ik}\right) M_{jl} + \frac{1}{\sin^2(x_i)} M_{ik}\frac{1}{h}T_{jl}.
\end{aligned}$$

Here T denotes the Toeplitz matrix (altered at the first and last row to account for the Neumann boundary condition)

$$T = \begin{pmatrix}
-1 & 1 & 0 & 0 & \cdots & \cdots & \cdots \\
1 & -2 & 1 & 0 & 0 & \cdots & \cdots \\
0 & 1 & -2 & 1 & 0 & 0 & \cdots \\
\vdots & \ddots & \ddots & \ddots & \ddots & \ddots & \vdots \\
\cdots & 0 & 0 & 1 & -2 & 1 & 0 \\
\cdots & \cdots & 0 & 0 & 1 & -2 & 1 \\
\cdots & \cdots & \cdots & 0 & 0 & 1 & -1
\end{pmatrix}$$

and S is the Toeplitz matrix

$$S = \begin{pmatrix}
0 & 1 & 0 & \cdots & \cdots \\
-1 & 0 & 1 & 0 & \cdots \\
\ddots & \ddots & \ddots & \ddots & \ddots \\
\cdots & 0 & -1 & 0 & 1 \\
\cdots & \cdots & 0 & -1 & 0
\end{pmatrix}.$$

These are the stiffness matrices of the one dimensional operators ∂_x^2 and ∂_x respectively. The mass matrix M is tridiagonal with $(1, 4, 1)/6$ on the diagonal and I denotes the identity. According to Definition 3.2 the discrete solution of the elliptic problem should satisfy

$$K\hat{u} = M\hat{f},$$

where $\hat{u}$ and $\hat{f}$ denotes the vector of coefficients in the basis $\phi_i(x) \otimes \phi_j(y)$. By "lumping" (replacing it by the identity) the mass matrix and dividing both sides by h we arrive at our discrete version of L_κ, in this basis given by the familiar looking matrix

$$L_h = \left(\frac{1}{h^2}T + \frac{1}{h\tan(x_i)}S\right) \otimes I + \left(\frac{1}{\sin^2(x_i)}I\right) \otimes \frac{1}{h^2}T.$$

Accidentally, these matrices coincides with the ones arising from a finite difference scheme. For tensor products of higher order splines there is a similar formula for the stiffness matrix as a Kronecker product of the one dimensional stiffness matrices.

Another fine property of the space $S^1 \otimes S^1$ is that the interpolation operator I_h

$$I_h(u) = \sum_{i,j} u(x_{ij})\phi_i\phi_j$$

is of optimal order as an approximation operator

$$I_h : H^s \to S^1 \otimes S^1,$$

in the sense that

$$\|u - I_h u\|_{L^2} \leq Ch^s \|u\|_{H^s} \quad 0 \leq s \leq 2.$$

In order to verify that the spatial discretization is correctly implemented we solve the Poisson equation on Ω with Neumann boundary conditions,

$$\begin{cases} (L + I)u = f & \text{in } \partial\Omega \\ \hat{n} \cdot \nabla u = 0 & \text{on } \partial\Omega \end{cases}, \tag{21}$$

for a suitable function f for which the exact solution is known. Thus, the exact error is plotted. As Figure 4 shows we have indeed second order convergence as expected.

4.2 Computing a reference solution

Since there are no nontrivial analytic solutions of the Meinhardt equations we will compute a reference solution as means of measuring the error when comparing different time stepping methods. The standard Crank-Nicolson method is well known to be second order convergent and unconditionally stable. Since the other methods are only first order in time and we are mainly interested in big step sizes, we can be confident that difference in the computed error and the real error is many orders of magnitude smaller than the real error.

When implementing Crank-Nicolson or implicit Euler it is necessary to solve a large system of nonlinear equations at each time step. For example, with two components on a 100×100 grid that would be a system of 20 000 nonlinear equations. This is done by an iterative process, Newton's algorithm. Thanks to the relative simplicity of the nonlinear term we can calculate the Jacobian analytically, which dramatically reduces the computational effort. Nonetheless, since the Jacobian involves the linearization of F at $u(t_n)$ which varies with time, one is forced to compute a new Jacobian for each time step. Usually each time step requires about two or three Newton iterations to get the residual below the tolerance level which we set to 10^{-9}.

We verify that the implementation of the Crank-Nicolson method is second order convergent by fixing a spatial grid and comparing the solution of for various step sizes with the numerical solution of a considerably smaller step size. Thus what is plotted is not the exact error but

$$\text{error}* = U_k(t_n) - U_{k^*}(t_{n*})$$

where $k^* = 10^{-6} << k$ and $t_n = kn = k^*n^* = t_n*$. The result can be seen i Figure 5.

By comparing the numerical solution of (18) on the 50x50 grid with that of a 150x150 grid we can estimate the semi-discrete error, that is, the error of the ODE (8) as an approximation

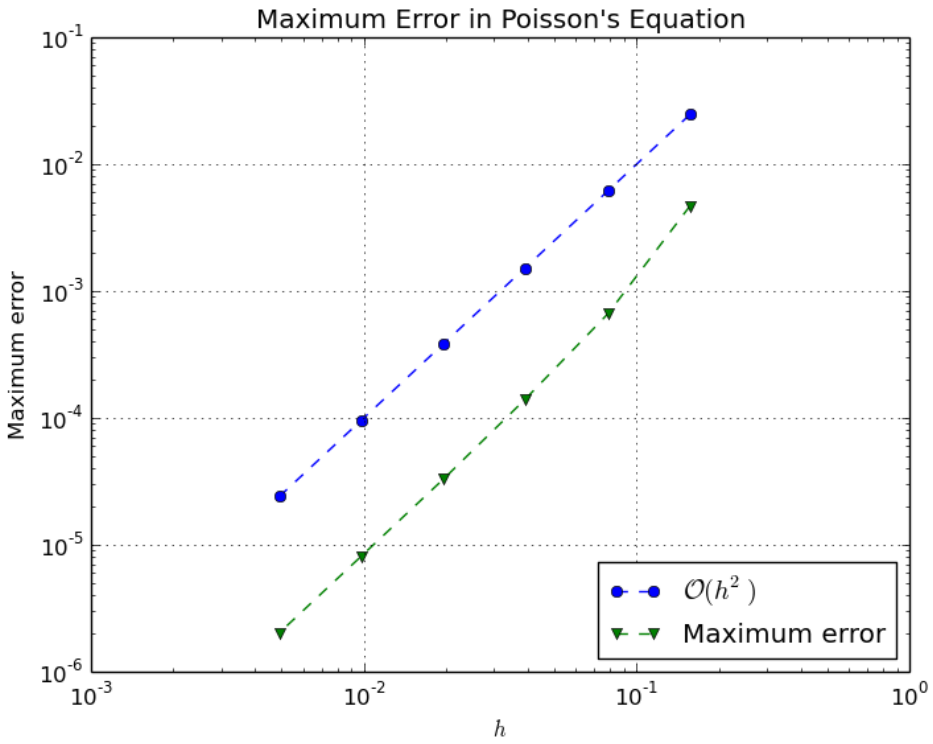

Figure 4: Second order convergence of Poisson's equation $(L+I)u = f$. We take $u(x,y) = \cos\left(\frac{\pi(x-x_0)}{\pi-x_0-x_1}\right)\cos(y))$ and apply $L+I$ (preferably in Maple or some other CAS) to obtain f. We then interpolate f to obtain $\hat{f}$, and solve the equation $(L_h+I)\hat{u} = \hat{f}$.

to the PDE (4). The result can be seen i Figure 5. Apparently the spatial error dominates for $k \leq 0.005$. Thus little is gained in decreasing k below 0.005 for a 50x50 grid. This once again emphasizes the inadequacy of explicit methods since for those, the CFL-condition alone requires $k \leq 10^{-6}$ and much smaller on a finer grid.

4.3 Stiffness of the nonlinear term

Since we in the splitting schemes will use explicit Euler to calculate the time evolution of the nonlinear term it is interesting to investigate its stiffness properties. For this purpose we apply explicit Euler to the corresponding ODE for various step sizes, see Figure 6. In general Explicit Euler is unstable for large step sizes. Of course IMEX will then have similar stability deficiencies when applied to the full problem, since the IMEX reduces to Explicit Euler in the spatially homogeneous case.

In contrast to explicit schemes there will be no CFL-condition on the IMEX method. This is since the instability is caused by the nonlinear term and not the diffusion. Thus it is the size of the solution rather than the spatial discretization that causes numerical instability.

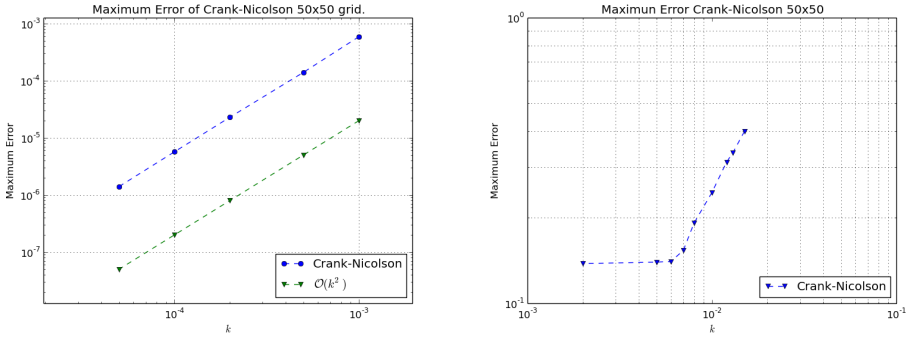

Figure 5: Convergence of the Crank-Nicolson scheme. We use the same parameters and initial values as in figure 3 and calculate until $t = 1$. Here the error is obtained by comparing against a numerical reference solution computed by the same scheme with $k = 10^{-6}$. We set the tolerance in the Newton iteration to 10^{-9}. Evidently the error vanishes of second order which gives us some confidence about the reliability of the reference solution. Next, we estimate the spatial error by comparing the solution on a 50x50 grid with that of a 150x150 grid. The error produced by the spatial discretization clearly dominates for $k < 0.005$.

It is possible to take several explicit steps for every implicit, thus at least eliminating the *numerical* instability. This does not rule out the possibility that the nonlinearity itself is unstable. It could be the case that the exact flow of the full equation

$$e^{k(L+F)}$$

is stable, while at the same time the exact flow of the nonlinearity

$$e^{kF}$$

blows up in k. To rule out this possibility a more careful analysis of the nonlinearity is required.

4.4 Efficiency experiments

In this section we compare the efficiency of the three time stepping methods introduced above. Of course this does not give a definitive answer of which algorithm is the best one since the performance depends on the implementation, hardware etc. The algorithms themselves could of course also be optimized in different ways, for example with some adaptive step size or by applying a method of higher order accuracy. Nonetheless, they are in some sense all "equally bad", and the results gives at least on a naive level some indication that the splitting schemes are very well suited for this type of problem.

The results can be seen in figure 9. It is clear that both IMEX and ADI are much more efficient than IE, which is already much more efficient than EE. Somewhat surprisingly however, the dimensional splitting is less efficient than IMEX, even though taking a time step with ADI is roughly twice as fast as with IMEX. This implies that the splitting error caused by the dimensional splitting is not negligible. This can be attributed to the fact stated earlier, that the operators $\partial_x^2 + \frac{1}{\tan(x)}\partial_x$ and $\frac{1}{\sin(x)^2}\partial_y^2$ do not commute, or more precisely the commutator is large on this domain.

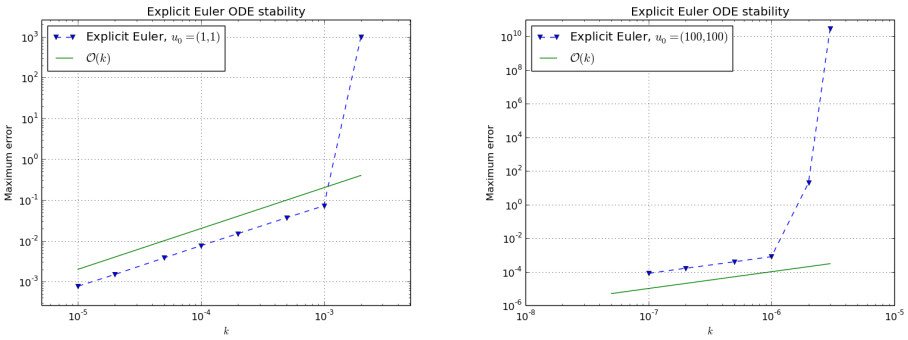

Figure 6: To the left Explicit Euler is applied to the nonlinear ODE $\partial_t u = F(u), u_0 = (1,1)$. It is clear that the numerical solution suffers from instability when $k > 10^{-3}$. To the right Explicit Euler is applied to the same ODE but with a larger initial datum, $u_0 = (100,100)$. The scheme is now unstable for $k > 10^{-6}$.

5 Conclusion

We have made a rigorous definition of a reaction diffusion system on a sphere and defined what we mean by a classical and weak solution. The existence, uniqueness and regularity of such solutions were then briefly discussed. While the question of global existence can be a delicate one, at least locally solutions always exists and typically possesses a high degree of regularity.

To start the numerical discussion we then introduced the Galerkin method for discretizing the spatial variable and proved some convergence rates. Next, the resulting ODE was discretized by a few different schemes and convergence rates was proved for the implicit Euler algorithm.

In the fourth section some numerical experiments were carried out with an activator-substrate model proposed by Geirer-Meinhardt. Basic lady beetle patterns such as spots and stripes were generated from simple initial values. We also backed up the theoretical convergence results with some numerical studies. The efficiency of the splitting schemes and implicit Euler were compared. While both the ADI and the IMEX splitting outperformed implicit Euler, it was IMEX that turned out to be the most efficient.

The work in this thesis can be furthered in many directions. It would for example be interesting to see how different parameterizations of the sphere affects the efficiency of the ADI splitting. Is it possible to make a decomposition of L such that the resulting matrices A_x and A_y are less "noncommutative", and there by reducing the splitting error? For the pure IMEX splitting one could experiment with taking several shorter explicit nonlinear steps for each linear implicit step and thus eliminating the stability deficiencies. Since the explicit step is much less costly than the implicit one, optimal efficiency would require that the splitting error and the implicit error dominates.

Another question is how other choices of S_h affects the efficiency. Given the high a priori regularity of the exact solution it is tempting to try to approximate it in some subspace with a higher order of approximation. However, by taking basis functions with larger support it gets more complicated to calculate the projection of the nonlinearity, $P_h F(u)$, at each time step. This is a question of computation rather than convergence.

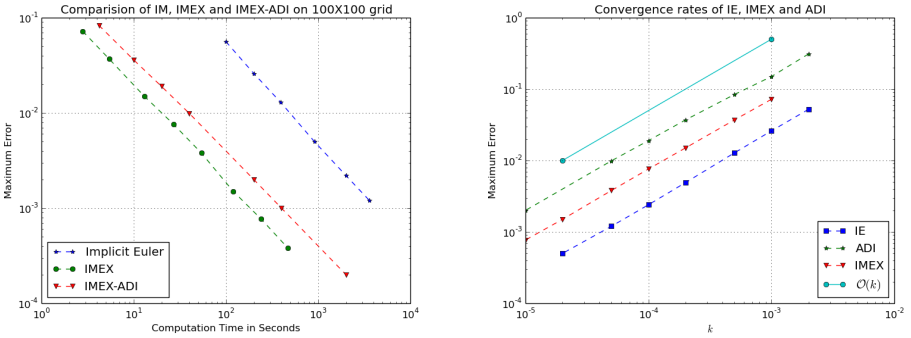

Figure 7: In the first figure we compare the efficiency of IE, IMEX and ADI on a 100x100 grid and $t_n = 1$. The same initial datum as in figure 1 is used. Clearly, IMEX performs best of the three methods. Next, not in completely reversed order, we have the convergence rates. While it is clear that all three methods are first order convergent, it is notable that the splitting itself introduces a considerable error. Perhaps not surprisingly ADI is also much more inaccurate than the simple IMEX, since we here also split the diffusion.

One would of course also want to address some questions related to the biological problem, preferable in connection with some empirical studies. This could involve making a more systematic numerical study of the parameters in the model. If for example the seven spot pattern can only be obtained from a very small region in the parameter space then this would indicate some unknown mechanism at work. Perhaps it is necessary splitting the domain in two, so that each wing develops independently. The model could of course be refined in many other ways such as considering growing domains or spatially dependent production rate of substrate. Ultimately the goal would be to identify not only the chemical components of the reaction, but also the full chain of genes involved. Quite possible the activator itself does not provide the pigmentation, rather it may trigger the cell to produce it. This of course constitutes an involved program, where even the slightest guidance from the kind of simulations presented in this thesis would be welcome.

References

[1] J. D. Murray, *Mathematical Biology II*, Springer-Verlag, third edition, 2003 Berlin Heidelberg.

[2] S. S. Liaw, C. C. Yang, R. T. Liu and J. T. Hong, *Turing model for the patterns of lady beetles*, Physical Review E, Vol.64.

[3] A. M. Turing, *The Chemical Basis of Morphogenesis*, Philosophical Transactions of the Royal Society of London Series B Vol. 237, (1952), pp.37-72.

[4] H. Meinhardt, *Models for the Generation and Interpretation of Gradients*, Cold Spring Harb Perspect Biol 2009; doi: 10.1101/cshperspect.a001362 originally published online July 15, 2009.

[5] H. Meinhardt, *Turings' theory of morphogenesis of 1952 and the subsequent discovery of the crucial role of local self-enhancement and long-range inhibition*, Interface Focus, doi: 10.1098/rsfs.2011.0097, originally published online 8 February 2012.

[6] L. C. Evans, *Partial Differential Equations*, AMS, Rhode Island 1998.

[7] S. C. Brenner, L. R.Scott, *The Mathematical Theory of Finite Element Methods*, Third Edition, Springer, New York 2000.

[8] V. Thomée, *Galerkin Finite Element Methods for Parabolic Problems*, Springer-Verlag, Berlin Heidelberg 1997.

[9] A. Pazy, *Semigroups of Linear Operators with Applications to Partial Differential Equations*, Springer-Verlag, New York 1983.

[10] M. Pierre, *Global Existence in Reaction-Diffusion Systems with Control of Mass: a Survey*, Milan Journal of Mathematics Volume 78, (2010), Issue 2, pp 417-455.

[11] J. A. Nietsche, A. H. Schatz, *Interior Estimatesfor Ritz-Galerkin Methods*, MATHEMATICS OF COMPUTATION, volume 28, number 128 october 1974, pages 937-958.

Bachelor's Theses in Mathematical Sciences 2016:K8
ISSN 1654-6229

LUNFNA-4009-2016

Numerical Analysis
Centre for Mathematical Sciences
Lund University
Box 118, SE-221 00 Lund, Sweden

http://www.maths.lth.se/